Available online at www.sciencedirect.com

ScienceDirect

Procedia CIRP 107 (2022) 1059–1064

www.elsevier.com/locate/procedia

55th CIRP Conference on Manufacturing Systems

Tri-Dexel Based Cutter-Workpiece Engagement Determination For Robotic Machining Simulator

Valentin Dambly*[a], Édouard Rivière-Lorphèvre[b], Olivier Verlinden[a]

[a]*Department of Theoretical Mechanics, Dynamics and Vibrations, University of Mons (UMons), Place du Parc 20, Mons 7000, Belgium*
[b]*Department of Machine Design and Production Engineering, University of Mons (UMons), Place du Parc 20, Mons 7000, Belgium*

* Corresponding author. Tel.: +3265374325. *E-mail address:* valentin.dambly@umons.ac.be

Abstract

In the spirit of digital twins, computer simulations is a crucial aspect for a technology. Within the frame of virtual manufacturing, and more precisely robotic machining simulation, this article aims to present a simulator developed in C++ for test purposes. It computes the machining forces and the update of the workpiece for 5-axis operations. The proposed method is based on the modelling of workpiece using multi-dexels with scalable resolution and a disk modelled tool with triangle-mesh surfaces. Chip thickness computation approaches are based on the interference between the dexel network with the surface swept by cutting edges either modelled as quadratic surfaces or planar swept surfaces coupled with a quadratic interpolation in the tool space, in the view of reducing computation time. Simulation results of both methods are compared with benchmark operations from the literature in terms of machining forces and with each other in terms of computation performances.

Keywords: Virtual machining; robotic machining; 5-axis milling; workpiece modelling; tri-dexels

1. Introduction

In the context of Industry 4.0 and its digital twins concept, virtual manufacturing has grown to become essential. As a matter of fact, this revolution was lead by the increasing efficiency of accurate approaches for the modelling of machine tool - workpiece interaction. The cutting conditions can be optimised to place the operation in a stable region by avoiding phenomena such as chatter vibrations, which is a current problematic met in robotic machining.

Robotic machining is a fast-growing technology in the field of mechanical manufacturing. Indeed, it is generally accepted that for the same working space, a fully equipped robotic machining cell can cost 30 to 50 % less than a conventional machine tool and enables agility to deal with complex workpieces [1]. However, for hard materials, inaccuracies occur due to the robot flexibility while subjected to cutting forces. To improve the accuracy of robotic machining operations, it has been shown that a significant part of the deviations, up to 80%, can be compensated offline by relying on faithful models of the operation.

In the context of model-based trajectory compensation, it is necessary to model the cutter-workpiece engagement (CWE) and the resulting forces along the tool while operating complex trajectories, in order to eventually couple them with dynamics simulator. The approaches proposed in this paper permit to accurately compute the machining forces for multi-dexel workpiece with tools modelled by triangle-mesh rake faces.

The paper first presents approaches to model the workpiece in view of interaction with a milling tool. Afterwards, the machining simulation principle is introduced with further details on the determination of the CWE for multi-dexel workpiece. The two approaches proposed for its determination are developed, validated against experimental results from benchmark operations and their computation times are compared as well as the ability to properly estimate the chip thickness and consequently the machining forces.

2. State of the art

Numerous modelling methods have been proposed to compute the CWE features since the breakthroughs in digital technologies [2]. The choice of the modelling method for the workpiece depends on the purpose of the simulation. For micro-

2212-8271
10.1016/j.procir.2022.05.108

mechanics simulation, with the aim of representing accurately the thermo-elastic behaviour of material, with chip deformation and friction along the cutting edge, finite-element method (FEM) is the appropriate candidate.

However, in the frame of this study, the focus is on the macro-mechanics since the main objective is to compute the machining forces at stake as well as the machined surface. Methods such as FEM are time consuming and not suited to the simulation of longer operations. Solid modelling methods are preferred for exact determination of machined surface with constructive solid geometry (CSG) approach where interactions are carried out with Boolean operations between elementary volumes. With a view of coupling the computation of forces with the dynamic simulation of cutting machine, the computation of the CWE and forces must be carried out at each time step [3]. Hence discrete modelling approaches are preferred such as dexel [4], voxel [5] and level curves [6].

The dexel approach is commonly accepted for workpiece modelling especially for five-axis milling operations [7, 8]. The intersection is computed between the workpiece and either the tool envelope [9, 10] or by considering the cutting edges motion. Denkena et al. demonstrated the efficiency of the latter and its flexibility regarding to various cutting situations such as interaction with block tools and tool with inserts [11, 12]. The dexel network can be coupled with analytical approaches such as Alpha shape to refine the determination of chip thickness [13, 14].

Further optimisation has been carried out for fast estimation of chip thickness, allowing real time computation, especially for inserts tools [15, 16]. In contrast with the later approach, the tool is discretised with triangular elements.

Nomenclature

CWE	Cutter-workpiece engagement
$d_{dex,i}$	Discretisation of dexel grid along i axis
$h_{k,j}$	Uncut chip thickness for slice k at tooth j
$HS_{i-1,i}(\xi)$	Hermite Spline between bounds $i-1$ and i
$\mathbf{K}_c$	The shear force coefficients
$\mathbf{K}_e$	The edge force coefficients
$\vec{p}$	position in $\mathbb{R}^3$
$\vec{p_d}$	position of a dexel point
$\vec{p_c}$	position of the cutting edge (generic expression, without specifying slice and tooth *nbr*)
$\vec{p_{k,j}}$	position of the cutting edge in slice k at tooth j
$\vec{p_{k,a}}$	position of the tool centre in slice k
$\mathbf{R}_{i,j}$	Rotation matrix from frame i to j ($\in SO_3$)

3. Machining simulation

Virtual manufacturing aims to simulate the material removal operations and the related phenomena. The mechanistic approach is used to model the operation at the macro-mechanical

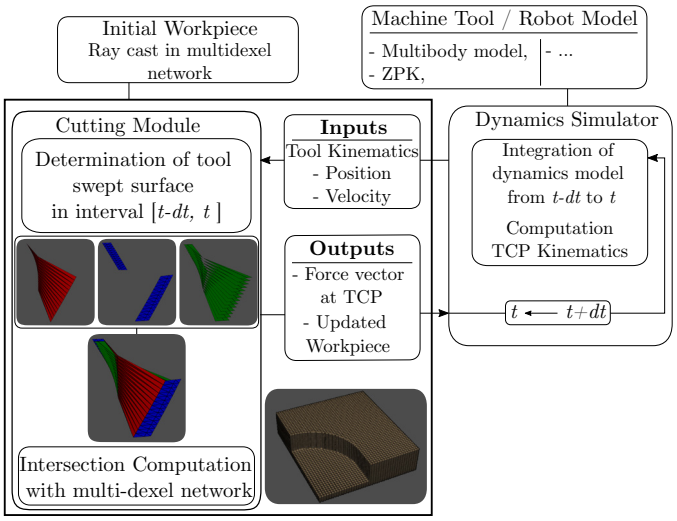

Fig. 1. Schematic representation of module input-output flow in simulation process. The visualisation of tool cutting edge swept surface as well as the workpiece is carried out with VTK through Pyvista [18].

level. The cutting module can be coupled with any other simulators of the dynamics of the machine. This module is initially developed for offline simulation of machining operation in order to assess operation stability and tool trajectory optimisation. The dexel approach is selected since intersection computation between tool and workpiece can naturally consider 5-axis operations as well as thank to the opportunity of efficient memory management. The module inputs are, apart from the tool geometry and simulation parameters, the workpiece, and kinematics of the tool at $t - dt$ and t with :

- $\vec{p}_{TCP}$: the tool centre point position
- $\mathbf{R}_{TCP}$: the orientation matrix of the tool
- $\vec{v}_{TCP}$: the tool centre point translational velocity
- $\vec{\omega}_{TCP}$: the tool centre point rotational velocity

The outputs of the module are the updated workpiece, based on intersection between cutting edges swept surface and multi-dexel model, and the instantaneous machining force at each time-step, based on the integration of elementary forces along cutting edges. The time-step value is chosen so that there are enough evaluation points to correctly estimate the machining forces [17]. The module interacts with the dynamical model of the machine tool during the integration process with the input-output flow presented in Figure 1. The force applied on the tool at time t correspond to the machining force computed during the time step $[t - dt, t]$.

Following the generally accepted approach [19], the tool is discretized in space as a slack of slices as depicted in Figure 2. The minimal amount of slices depends on the helix angle.

The machining force is computed as the sum of the elementary contribution of each slice where this contribution $d\vec{F}$ is determined with the mechanistic approach :

$$dF_i = \mathbf{K}_{i,c} \cdot h \cdot dz + \mathbf{K}_{i,e} \cdot dS \tag{1}$$

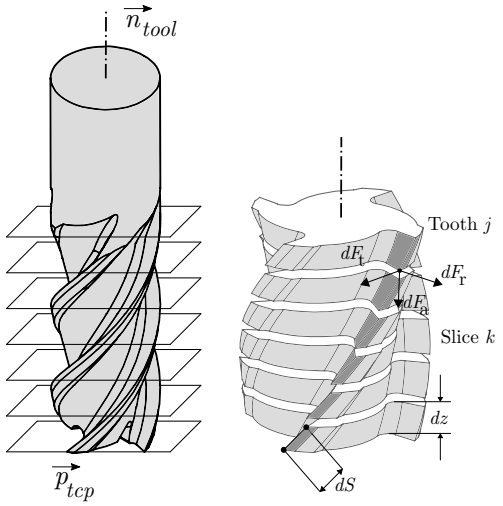

Fig. 2. Slack of slices modelling of a milling tool.

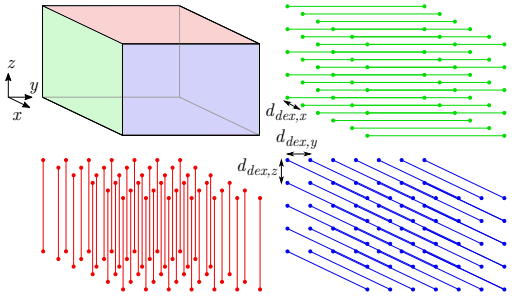

Fig. 3. Representation of a block with tri-dexel approach.

with $i = t, r, a$ being the tangential, radial and axial directions, h the chip thickness, dz the height of the slice and dS the edge length. The shear force and edge coefficients $\mathbf{K}_{i,c}$, $\mathbf{K}_{i,e}$ are identified experimentally. The key element to estimate in Equation 1 is the chip thickness h, resulting from the evaluation of the CWE.

4. Cutter-workpiece engagement

The CWE results form the intersection between the tool and the workpiece. For the specifications of the simulation, the workpiece is modelled with tri-dexel approach. It consists in representing the matter as a network composed of three sub-networks of lines going along each of the global directions x, y, z as depicted in Figure 3. A dexel is a uni dimensional element holding segments of matter. The sub-network of dexels along the x direction is defined in the $y-z$ plane with dexels placed with discretisation steps $d_{dex,y}$, $d_{dex,z}$ along these directions (Figure 3).

As justified in the previous section, it is relevant to consider the stack of slice tool model for forces estimation. The intersection must then be computed slice-wise. For the slice k, three surfaces are considered to compute the intersection with the dexel network (Figure 4). The motion of a slice between two time-steps is illustrated in Figure 4, with the corresponding surfaces (S_1,S_2,S_3):

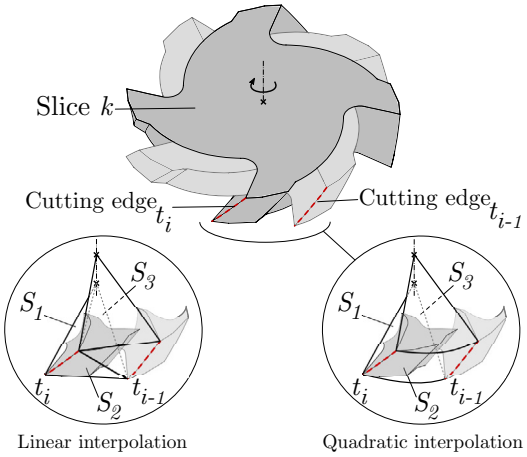

Fig. 4. Discretization in time of the cutting edge motion for the slice k with discretization of the swept surface using either linear interpolation (left) or quadratic interpolation (right).

- the first surface (S_1) represents the cutting edge at time t_i, it is composed of the cutting edge corners and tool axis points;
- the second surface (S_2) represents the surface swept by the cutting edge during the time interval $[t_{i-1}, t_i]$;
- the third surface (S_3) represents the bottom of the slice, since the slices are stacked, it is necessary to take this surface into account to properly update the dexel network while processing the stacks. It is only used for the network update and not chip thickness computation (cfr. Section 4.2).

Two approaches to consider these surfaces and their use for uncut chip thickness computation are described in the following part of the section. These approaches being either the linear or quadratic interpolation of tool motion between consecutive time-steps.

4.1. Planar swept surface

For small time-step, the angle covered by the cutting edge can be small enough to consider a linear interpolation of this cutting edge for 2.5D operations with layered representation of workpieces [20]. This approach has been extended for tri-dexel workpieces [21].

Each of the surfaces (S_1, S_2, S_3) is defined by two triangles. This elementary discretisation is represented in the "Linear Interpolation" bubble in Figure 4. The computation of the intersection between dexels and swept surface is straightforward and low time consuming. With the aim of reaching an accurate determination of the chip thickness, it is proposed to decouple its determination from the intersection computation. Instead, it is computed based on the generation of the local machined surface from the tool motion.

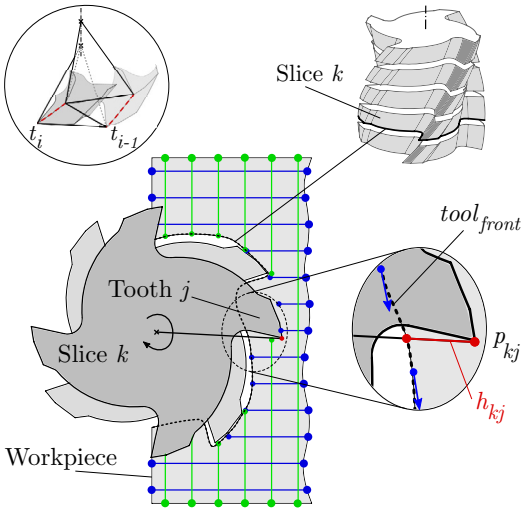

Fig. 5. Illustration of the uncut chip thickness h_{kj} computation at slice k for tooth j with the planar swept surface approach coupled with the Hermite interpolation of previous cutting edges positions $tool_{front}$.

The machined surface can be considered as the surface delimited by the cutting edges positions that did cut the dexel network and the workpiece boundaries. In order to determine the chip thickness $h_{k,j}$ for slice k, tooth j, the distance between the cutting edge point $p_{k,j}$ and the former machine surface is computed, as shown in Figure 5. The front of matter corresponds to the previous tool positions that cut the dexel network, and then coincides to the tool front ($tool_{front}$ in Figure 5). Since the kinematics of the tool is known, for each slice, these cutting edge positions and velocities are stored and used to generate the boundary with Hermite splines as depicted with the dashed line in Figure 5. The Hermite spline is defined as follows:

$$\vec{p}_{tool_{front}}(\xi) = HS\left(\begin{pmatrix}\vec{p}_{c,b}\\ \vec{v}_{c,b}\end{pmatrix}_{i-X}, \begin{pmatrix}\vec{p}_{c,b}\\ \vec{v}_{c,b}\end{pmatrix}_{i-1}\right)(\xi) \tag{2}$$

with ξ the interpolation parameter, subscript b the **b**ottom cutting edge points of the slice and X the amount of previous stored cutting edge points necessary for a full revolution of the tool. The determination of the CWE can be considered hybrid since the intersection with the workpiece is based on the interaction with the dexel network and the chip thickness computation relies on the aforementioned approach.

This hybrid CWE computation method implies that $h_{k,j}$ does not exclusively rely on the intersections with the dexel network. It only needs the detection of an interference between a dexel and the tool, enabling to accept less strict dexel resolution d_{dex}.

4.2. Quadratic swept surface

The surface swept by the cutting edge during the time interval $[t_{i-1}, t_i]$ can be modelled as a quadratic surface. Since the aim is to compute the machining forces along the tool, the slack of slices discretisation shown in Figure 2 is conserved.

As for the linear interpolation case, the same three surfaces are considered, except that they are generated with quadratic functions. Indeed, the input of the module being the tool kinematics, the cutting edges points positions ($\vec{p}_{k,j}(t_{i-1})$, $\vec{p}_{k,j}(t_i)$) and velocities ($\vec{v}_{k,j}(t_{i-1})$, $\vec{v}_{k,j}(t_i)$) are known for each slice k and tooth j as well as the tool axis points positions ($\vec{p}_{k,a}(t_{i-1})$, $\vec{p}_{k,a}(t_i)$) and velocities ($\vec{v}_{k,a}(t_{i-1})$, $\vec{v}_{k,a}(t_i)$).

From this information, Hermite splines are defined to interpolate the motion of the cutting edge between the evaluation times t_{i-1} & t_i. To illustrate the intersection computation, the case of the second surface S_2 is expressed afterwards in details. The second swept surface holds two parameters (μ, ξ) where μ represents the displacement along the cutting edge line between the two consecutive slices (red dashed line in Figure 6) with

$$\vec{p}_c(\mu, \xi) = \vec{p}_{c,b}(\xi) + \mu.(\vec{p}_{c,t}(\xi) - \vec{p}_{c,b}(\xi)) \tag{3}$$

the subscripts b and t denote the **b**ottom and **t**op cutting edge points of the slice and ξ represents the spline parameters corresponding to the progression of the cutting edge in the time interval $[t_{i-1}, t_i]$.

$$\vec{p}_{c,b}(\xi) = HS\left(\begin{pmatrix}\vec{p}_{c,b}\\ \vec{v}_{c,b}\end{pmatrix}_{i-1}, \begin{pmatrix}\vec{p}_{c,b}\\ \vec{v}_{c,b}\end{pmatrix}_{i}\right)(\xi) \tag{4}$$

The intersections between the dexel network and the surface swept by the tooth j of slice k is a root finding problem expressed as follows:

$$\vec{f}(\mu, \xi, \eta) = \vec{p}_c(\mu, \xi) - \vec{p}_d(\eta) = 0 \tag{5}$$

with $\vec{p}_d(\eta)$ the point along the dexel line.

The problem presented in Equation 5 is solved using a Newtonian method with initial values $(\mu, \xi, \eta)_{initial}$ obtained by using the planar swept surface described in section 4.1.

With the swept surface interpolated with a quadratic surface, the chip thickness can be computed directly using the dexels and the surface. The chip thickness $h_{k,j}$ depends on the surface that has cut the dexel as depicted in Figure 6. As mentioned in Section 4, only the two first surfaces are considered. If the dexel is cut by S_1, the local chip thickness is the distance between the intersection and its projection on the cutting edge. If the dexel is cut by S_2, the dexel node inside the swept volume is projected on the swept surface and the distance between itself and its projection gives the local chip thickness. Finally, its value for the slice k tooth j is considered as the maximum of the local chip thickness values.

With this approach $h_{k,j}$ depends on the amount of dexel cut by S_1 and S_2, which implies that there is a minimal number of intersections to reach an acceptable chip thickness estimation.

5. Experimental validation with benchmark operations

The approach have been tested on two benchmark cases from literature with the half-immersion face milling operation of a four-teeth flat-end mill in Ti6Al4V and the slotting operation in GGG70 with a two-flute ball-end tool. The simulation parameters are presented in Table 1. Both cases were simulated for 60 tool rotations.

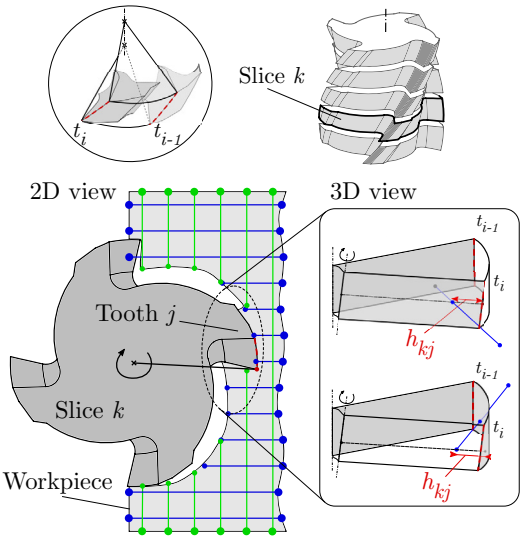

Fig. 6. Illustration of the uncut chip thickness $h_{k,j}$ computation at slice k for tooth j with the quadratic swept surface approach.

Table 1. Tool and simulation parameters for the comparison between the dexel-based simulator with quadratic and planar implementation and experimental data [22, 19].

		Case 1	Case 2
Workpiece Material		Ti6Al4V	GGG70
		Tool parameters	
Material		WC with TiAlON coated	Carbide
Diameter	$[mm]$	18.1	12
N° of edges (flutes)		4	2
Pitch/run out	$[°]/\mu m$	-/-	-/-
Helix angle	$[°]$	30	30
Number of slices		19	11
		Simulation parameters	
Rotation Speed	$[RPM]$	528	1000
Tooth feed	$[mm/tooth]$	0.05	0.08
Axial depth	$[mm]$	5.08	2
Operation type		Half-immersion	Slotting
$K_{t/r/a,c}$	$[MPa]$	1731/317/-623	2172.1/848.9/725.1
$K_{t/r/a,e}$	$[N/mm]$	24/43/0	17.3/7.8/6.6

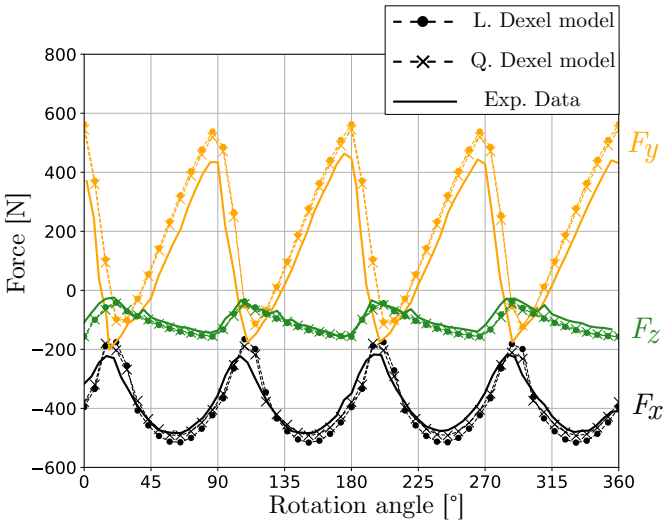

Fig. 7. Machining forces comparison for the planar intersection method (L. Dexel model), the quadratic surface based intersection method (Q. Dexel model) and experimental data (from [22]) over one tool rotation for a half-milling operation with a flat-end mill in Ti6Al4V.

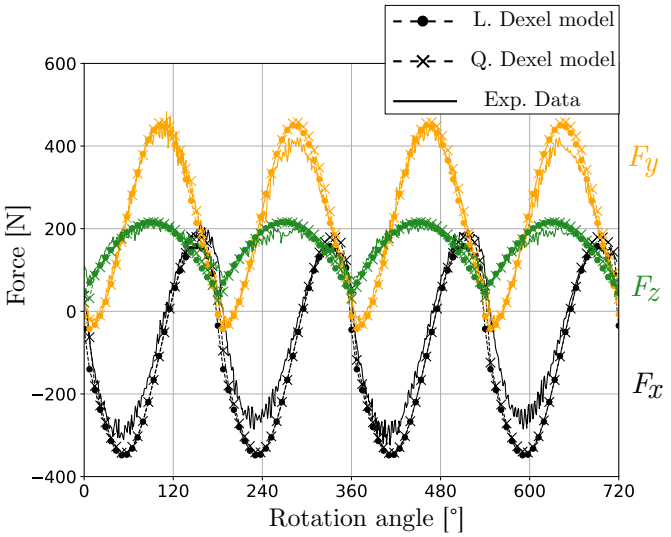

Fig. 8. Machining forces comparison between the planar intersection method (L. Dexel model), the quadratic surface based intersection method (Q. Dexel model) and experimental data (from [19]) over two tool rotations for a slotting operation with a ball-end mill in GGG70.

The two approaches are compared in terms of machining forces evaluation in Figures 7 and 8. For the ball-end case, a slight shift is noticed in the measurement for lower and upper forces along x and y directions respectively. This can be explained by an unidentified angle shift between the teeth or a potential run-out in the tool.

For both methods, the simulations estimate the forces at stake during the operation. It is however necessary to mention that the machined surface as well as the computation time differ. The machined surface estimation is, as one can imagine, more realistic with the quadratic interpolation. Nevertheless, the method presented in Section 4.1 presents an important gain in terms of computation time, since intersections are straightforward to compute. As an order of magnitude, the case 2 from Table 1 has been simulated for $3s$ operation time with a range of discretisation step $d_{dex,x} = d_{dex,y} = d_{dex,z}$, representing 8000 dexels. The comparison is made in terms of time and accuracy of the chip thickness evaluation (”Acceptable” criterion) and is presented in Table 2. This criterion is the image of the chip thickness computation by considering the evaluation acceptable if the chip thickness for each slice is within 5% estimation range with respect to the theoretical chip thickness profile. As shown in Table 2, the planar approach requires a less dense dexel network than the quadratic approach since the later directly relies on the dexels cut by the swept surface. For planar approach, going beyond the ”Limit” means that the dexels are too spaced from each other and cutting edges motion might not detect matter anymore. The hybrid planar-analytical method allows a fast computation of the machining forces with a discrete modelling

method for workpiece. It enables to simulate the dynamics of 5-axis operations with machine tools as well as machining robots.

Table 2. Comparison of computation time and validity of chip thickness evaluation with respect to the discretisation step used for the dexel model of the workpiece. The simulations are carried out on a Intel Core i7-10850H - 2.7GHz.

Op. time	3 [s]	L. Dexel Model		Q. Dexel Model	
d_{dex} [m]	N_{dexels}	time [s]	Acceptable	time [s]	Acceptable
$2e^{-4}$	4567	39.1	Yes	6145	Yes
$2.5e^{-4}$	2999	26.05	Yes	3561	Yes
$3e^{-4}$	2069	17.8	Yes	2081	No
$3.5e^{-4}$	1527	16.2	Limit	/	/

6. Conclusion

The article presents a machining simulator module that can be coupled with machine tool dynamics simulator. This module computes the machine forces at each time step and updates the machined surface. Two approaches have been presented with the planar swept surface used for the workpiece update coupled to a chip thickness determination based on the tool previous positions and the quadratic swept surface used for both surface update and chip thickness computation.

The approaches described enable to compute reliable machining forces as well as machined surface for workpiece modelled with a tri-dexel network. The tool and workpiece are decoupled, enabling simulations of 5-axis operations, which are commonly met in robotic machining. Since the forces are computed time-step wise, the simulator can be coupled with a solver for machine tool dynamics.

Both methods showed an accurate estimation of the machining forces. However, the planar approach coupled with the exact chip thickness evaluation lades to a faster estimation of the machine forces for an equivalent accuracy.

Future work is being considered with the modelling of 5-axis trajectories as well as the coupling with complex systems such as machining robots to assess the stability of the operation and selection of optimal cutting parameters. Also, the chip thickness computation for the quadratic approach must be optimised to reach a smaller computation time. With further optimisation, shorter simulation time can be achieved, enabling online applications of force estimation.

Acknowledgements

The authors would like to acknowledge the Belgian National Fund for Scientific Research (FNRS-FRS) for the grant allotted to V. Dambly.

References

[1] A. Verl, A. Valente, S. Melkote, C. Brecher, E. Ozturk, T. Tunc, Robots in machining, CIRP Annals (2019) 799–822.

[2] Y. Altintas, P. Kersting, D. Biermann, E. Budak, B. Denkena, I. Lazoglu, Virtual process systems for part machining operations, CIRP Annals - Manufacturing Technology 63 (12 2014).

[3] J. Bauer, M. Friedmann, T. Hemker, M. Pischan, C. Reinl, E. Abele, O. Von Stryk, Analysis of Industrial Robot Structure and Milling Process Interaction for Path Manipulation, Springer, 2013, pp. 245–263.

[4] V. Böß, C. Ammermann, D. Niederwestberg, B. Denkena, Contact zone analysis based on multidexel workpiece model and detailed tool geometry representation, Procedia CIRP 4 (2012) 41–45.

[5] I. Nishida, R. Okumura, R. Sato, K. Shirase, Cutting force and finish surface simulation of end milling operation in consideration of static tool deflection by using voxel model, Procedia CIRP 77 (2018) 574–577.

[6] V. Böß, B. Denkena, B. Breidenstein, M.-A. Dittrich, H. N. Nguyen, Improving technological machining simulation by tailored workpiece models and kinematics, Procedia CIRP (2019) 224–230.

[7] M. Inui, N. Umezu, Cutter engagement feature extraction by using dexel representation solid model, Key Engineering Materials 523-524 (2012) 420–432.

[8] Y. Boz, H. Erdim, I. Lazoglu, A comparison of solid model and three-orthogonal dexelfield methods for cutter-workpiece engagement calculations in three- and five-axis virtual milling, The International Journal of Advanced Manufacturing Technology 81 (05 2015).

[9] M. Inui, M. Kobayashi, N. Umezu, Cutter engagement feature extraction using triple-dexel representation workpiece model and gpu parallel processing function, Computer-Aided Design and Applications 16 (2019) 89–102.

[10] J. Theegarten, D. Plakhotnik, M. Stautner, Z. Kilic, E. Berckmann, Y. Murtezaoglu, Discrete cutter-workpiece engagement for five-axis milling using tri-dexel model, Virtual Machining Process Technologies (04 2019).

[11] B. Denkena, T. Grove, O. Pape, Optimization of complex cutting tools using a multi-dexel based material removal simulation, Procedia CIRP 82 (2019) 379–382.

[12] B. Denkena, A. Kroedel, O. Pape, Increasing productivity in heavy machining using a simulation based optimization method for porcupine milling cutters with a modified geometry, Procedia Manufacturing 40 (2019) 14–21.

[13] S. Luo, Z. Dong, M. Jun, Chip volume and cutting force calculations in 5-axis cnc machining of free-form surfaces using flat-end mills, The International Journal of Advanced Manufacturing Technology 90 (04 2017).

[14] B. W. Peukert, A. Archenti, A modular node-based modeling platform for the simulation of machining processes, euspen's 21st International Conference & Exhibition, Copenhagen (2021) 351–354.

[15] B. Denkena, O. Pape, A. Kroedel, V. Böß, L. Ellersiek, A. Muecke, Process design for 5-axis ball end milling using a real-time capable dynamic material removal simulation, Production Engineering 15 (11 2020).

[16] B. Denkena, A. Kroedel, O. Pape, A. Muecke, L. Ellersiek, Identification of rake and flank face engagement parameters using a dexel-based material removal simulation with an oriented sweep volume, CIRP Journal of Manufacturing Science and Technology 35 (2021) 146–157.

[17] E. Rivière-Lorphèvre, H. Hoai Nam, O. Verlinden, Influence of the time step selection on dynamic simulation of milling operation, The International Journal of Advanced Manufacturing Technology 95 (2018) 1–16.

[18] C. B. Sullivan, A. Kaszynski, PyVista: 3D plotting and mesh analysis through a streamlined interface for the Visualization Toolkit (VTK), Journal of Open Source Software 4 (37) (2019) 1450.

[19] S. Engin, Y. Altintas, Mechanics and dynamics of general milling cutters Part I: Helical end mills, International Journal of Machine Tools and Manufacture 41 (2001) 2195–2212.

[20] H. N. Huynh, E. Rivière-Lorphèvre, F. Ducobu, A. Ozcan, O. Verlinden, Dystamill: a framework dedicated to the dynamic simulation of milling operations for stability assessment, The International Journal of Advanced Manufacturing Technology 98 (5) (2018) 2109–2126.

[21] V. Dambly, H. N. Huynh, O. Verlinden, E. Rivière-Lorphèvre, Development of tri-dexel based cutting simulator for cutter-workpiece engagement and cutting forces determination, euspen's 21st International Conference & Exhibition, Copenhagen (2021) 399–402.

[22] Y. Altintas, P. Lee, A general mechanics and dynamics model for helical end mills, CIRP Annals - Manufacturing Technology 45 (1996) 59–64.